01 Jan 2013

Modeling of the Resilient Modulus for Recycled Asphalt Pavement Applications in Base Course Layers

Ehab Noureldin

Magdy Abdelrahman
Missouri University of Science and Technology, abdelrahmanm@mst.edu

Recommended Citation
E. Noureldin and M. Abdelrahman, "Modeling of the Resilient Modulus for Recycled Asphalt Pavement Applications in Base Course Layers," *Transportation Research Record*, no. 2371, pp. 121-132, National Research Council (U.S.), Jan 2013.
The definitive version is available at https://doi.org/10.3141/2371-14

Modeling of the Resilient Modulus for Recycled Asphalt Pavement Applications in Base Course Layers

Ehab Noureldin and Magdy Abdelrahman

The resilient modulus (M_R) is an important parameter for the base course layer in the pavement design process. Use of recycled asphalt pavement (RAP) for this layer must take into consideration the effect of various factors that may occur in the field on the M_R. Previous numerical models used for the granular base layer could be used for the RAP. The study reported here examined the suitability of RAP procedures under the effect of different factors (e.g., water content, dry density, freeze–thaw cycles). Various percentages of the RAP (50%, 75%, and 100% by weight) were employed in this research. All the models included in the study took into account the effect of state of stresses directly, but they also considered the other factors mentioned and the effect of their interactions with the M_R indirectly. The intent of the study was twofold: (*a*) to determine the adequacy of the models employed in the use of the RAP procedure in the base course layer and (*b*) to determine which model best described RAP behavior under the effects of the tested factors. On the basis of a review of the literature, nine prediction models were chosen to investigate the granular base course layers so as to predict M_R for RAP. A pilot analysis was made of these models to compare the measured and predicted values of M_R under the tested factors. Three models showed a good prediction for the M_R. These three models were reassessed in a sensitivity analysis on regression parameters to choose the best-fit model for the RAP applications.

The paving industry faces tremendous problems worldwide because of the severe shortage of suitable aggregates in general and the high cost of virgin aggregates used in the pavement layers. Use of the recycled asphalt pavement (RAP) concept to construct an adequate granular base course layer is an excellent alternative, especially in cases in which the lack of suitable aggregates exists. FHWA reported that about 100 million tons of RAP are produced each year during pavement rehabilitation activities, which presents a major solid waste concern and consequential environmental pollution and hazards (*1*).

The resilient modulus (M_R) of unbound layers is a required property during any mechanistic or mechanistic–empirical analysis procedure for flexible pavements. The M_R test is a commonly conducted laboratory procedure to characterize the stiffness and elasticity responses of the base material (*2*). Proper characterization of the nonlinear, stress-dependent behavior of pavement unbound layers has a significant impact on the accuracy of pavement response predictions (*3*). The M_R of unbound granular material is affected by several factors, including the state of stress, moisture content, dry density, and freeze–thaw (F-T) action. Although several researchers have tried to understand and model the effect of these factors on the M_R of different granular materials, limited effort has been made to understand the effect of those factors on the M_R of RAP and RAP–aggregate blends as a pavement base course layer.

Several constitutive models have been investigated for their suitability to model the behavior of granular materials and RAP (*4*). However, these models were tested on RAP at different state of stresses and did not take into consideration other factors in the blend (e.g., moisture content, percentage of RAP). The main objective of these models was to choose the best alternative that described the behavior of RAP in the base layer under the effect of the most common field conditions. It also is important to know the optimum percentage of RAP in the blend, which simultaneously gives the best prediction of the M_R of the base course layer. These prediction models should, in any case, be compared at different percentages of RAP mixed in the blend under the effects of the field conditions mentioned.

BACKGROUND

The M_R is the main engineering property that describes the performance of base course materials (*5*). As pavements are subjected to repeated wheel loads, static testing procedures usually are not adequate to determine the behavior of aggregate materials subjected to dynamic load conditions. A number of methods are available to test the M_R. The most common protocols for this testing are AASHTO T 292-91, AASHTO T 294-92, AASHTO T-307, AASHTO T P46-94, LTPP protocol P46, and NCHRP 1-28 (*6*). During the M_R test, the sample is subjected to different levels of confining pressures and deviator stresses.

In this study, the samples were tested according to NCHRP 1-28.

The RAP is generated when asphalt pavements are removed for reconstruction, resurfacing, or to obtain access to buried utilities. Rehabilitation projects of old asphalt pavements produce a significant amount of RAP (*7*). FHWA reported that agencies in at least 13 states (i.e., Arizona, Illinois, Louisiana, Maine, Nebraska, New Hampshire, North Dakota, Oregon, Rhode Island, South Dakota, Texas, Virginia, and Wisconsin) had used RAP as an aggregate in the base layer (*1*).

On the basis of a review of the literature, nine prediction models have been used for granular base materials and tested on RAP and RAP–aggregate blends but only under the effect of different state of stresses. A summary of the investigated models is presented in Table 1. The M_R for granular material was found to increase with

Department of Civil and Environmental Engineering, North Dakota State University, CIE 201F, Fargo, ND 58105. Corresponding author: M. Abdelrahman, m.abdelrahman@ndsu.edu.

Transportation Research Record: Journal of the Transportation Research Board, No. 2371, Transportation Research Board of the National Academies, Washington, D.C., 2013, pp. 121–132.
DOI: 10.3141/2371-14

TABLE 1 ***M_R* Predictive Models**

Model Name	Equation
Confining pressure	$M_R = K_1 \cdot P_a \cdot \left(\frac{\sigma_3}{P_a}\right)^{K_2}$
Bulk stress	$M_R = K_3 \cdot P_a \cdot \left(\frac{\theta}{P_a}\right)^{K_4}$
Bulk and deviator stress	$M_R = K_5 \cdot P_a \cdot \left(\frac{\theta}{P_a}\right)^{K_6} \cdot \left(\frac{\sigma_d}{P_a}\right)^{K_7}$
Bulk and octahedral shear stress	$M_R = K_8 \cdot P_a \cdot \left(\frac{\theta}{P_a}\right)^{K_9} \cdot \left(\frac{\tau_{oct}}{P_a}\right)^{K_{10}}$
Pezo	$M_R = K_{11} \cdot P_a \cdot \left(\frac{\sigma_3}{P_a}\right)^{K_{12}} \cdot \left(\frac{\sigma_d}{P_a}\right)^{K_{13}}$
Average stress	$M_R = K_{14} \cdot \left(\frac{P}{\sigma_d}\right)^{K_{15}}$
General stress	$M_R = K_{16} \cdot P_a \cdot \left(\frac{\theta}{3P_a}\right)^{K_{17}} \cdot \left(\frac{\sigma_3}{P_a}\right)^{K_{18}} \cdot \left(\frac{\sigma_d}{P_a}\right)^{K_{19}}$
MEPDG	$M_R = K_{20} \cdot P_a \cdot \left(\frac{\theta}{P_a}\right)^{K_{21}} \cdot \left(\frac{\tau_{oct}}{P_a}+1\right)^{K_{22}}$
Witczak	$M_R = K_{23} \cdot P_a \cdot \left(\frac{\theta - 3K_{26}}{P_a}\right)^{K_{24}} \cdot \left(\frac{\tau_{oct}}{P_a}+K_{27}\right)^{K_{25}}$

NOTE: MEPDG = *Mechanistic–Empirical Pavement Design Guide*. In all the models, stress terms are normalized with respect to atmospheric pressure (P_a) where
σ_d = deviator stress (psi), ($\sigma_d = \sigma_1 - \sigma_3$),
σ_1 = axial stress (psi),
σ_2 = lateral stress (psi), ($\sigma_2 = \sigma_3$),
σ_3 = confining pressure (psi),
θ = bulk stress (psi) = $\sigma_1 + \sigma_2 + \sigma_3 = \sigma_d + 3\sigma_3$ (psi),
P_a = atmospheric pressure = 14.7 (psi) = 101.5 (kPa),
P = mean normal stresses = $\frac{(\sigma_1 + \sigma_2 + \sigma_3)}{3} = \frac{\sigma_d}{3} + \sigma_3$ (psi)
τ_{oct} = octahedral shear stress = $\frac{1}{3}\sqrt{\left\{(\sigma_1-\sigma_2)^2 + (\sigma_1-\sigma_3)^2 + (\sigma_2-\sigma_3)^2\right\}}$ (psi)
K_i = multiple regression constants evaluated from resilient modulus tests.

the increase in the confining pressure, as presented in the first model (*8*). Several researchers reported that the M_R value depended on the bulk stress θ (first stress invariant) applied to the sample. The *K*–θ Model was used to describe the resilient behavior of unbound material, as presented in the second model in Table 1. In reality, most soils are affected by the confining pressure and the shear stress. Uzan proposed a model that accounted for the shear stress effects (*9*). Uzan's model is presented as the third model in Table 1.

Later the octahedral shear stress was used instead of deviator stress, as presented in the fourth model (*10*). The M_R also was modeled on the basis of the deviator stress and confining pressure by Pezo, as presented in the fifth model (*11*). Tam and Brown suggested modeling the M_R of granular material with the mean stress to deviator stress ratio, as presented in the sixth model (*12*). Itani developed a model that included bulk stress, shear stress, and an additional confining pressure component, as presented in the seventh model in Table 1 (*5*). A modified form of Uzan's equation (*9*) is used in the *Mechanistic–Empirical Pavement Design Guide* (MEPDG), as presented in Table 1. Witczak evaluated 14 constitutive models in log-log and semilog forms for their capabilities to predict the resilient behavior of different granular material and recommended a five-parameter model that statistically had the overall goodness of fit (*13*). Witczak's Model is presented in Table 1.

PROBLEM STATEMENT

From the literature survey, it was clear that these prediction models were tested on RAP as a base course layer but under only one factor: the state of stresses, such as confining pressure, deviator stress, and bulk stress. The tests did not take into consideration other factors, such as water content, dry density, or environmental changes such as F-T conditions. Attia tested these models at different percentages of RAP research (*4*). However, the linear comparisons of the measured and predicted values of M_R were tested without consideration of the effect of the variation of other factors (e.g., water content, dry density, F-T cycles) at different percentages of RAP. Attia considered only the measured M_R at optimum moisture content (OMC) and maximum dry density (MDD) for different percentages of RAP. According to the literature, no parametric analysis has been made of these prediction models to understand the behavior of each multiple regression constant *K* parameter under different testing conditions. Thus it was important to assess whether each model fit for all tested conditions or if there was a need to test more field conditions (e.g., environmental impact factors).

RESEARCH OBJECTIVE

The main objective of this research was to assess the constitutive models previously tested for RAP as a base layer under the effect of different, actual environmental and field conditions other than the state of stresses. This objective was fulfilled in two stages. The first stage aimed to investigate the accuracy of these models by statistical analysis to show how they might be affected by the new conditions alone or in conjunction with various interactions at different percentages of RAP on the prediction of the M_R. The second stage was tailored to a parametric analysis of the best statistical models determined from the first stage to choose the one that best fit and its suitability to predict the M_R of RAP. If no model was suitable, it would be necessary to develop a new prediction model in the future. The study also assessed the adequacy of these factors to represent most of the field conditions that affected the base layer and then to investigate the need for more laboratory measurements to consider the effect of other environmental and field conditions to predict the M_R for the RAP mixes to be used in the base course layers (e.g., leaching contents of RAP).

RESEARCH METHODOLOGY

The known constitutive models for granular material were investigated for their suitability in the modeling of M_R behavior of RAP materials and mixtures. Each predictive model was run to predict the measured M_R values from laboratory tests conducted on RAP under different conditions and percentages. For each model, a multiple regression comparison was used for all levels (values) of stresses at various testing conditions and different RAP percentages, together with their interactions to determine the multiple regression factors (*K* constants) with use of the Excel solver.

With the use of Minitab software, a linear regression comparison then was made for each model of the predicted and measured M_R at all tested conditions. This procedure was used to calculate all regression-related parameters, such as R^2. Each prediction model was evaluated at a different RAP percentage, which varied from 50% to 100% for each tested condition or interaction between these conditions.

Finally, the best model was selected through a comparison of each of the K constants calculated from the multiple regression stage; all testing conditions took into consideration the RAP percentages 50%, 75%, and 100%. The study also estimated the optimum percentage or range of RAP values that gave the most accurate prediction for the M_R. The study also investigated any relationships that might have existed between each of the K values and the tested conditions.

EXPERIMENTAL CONSIDERATIONS

This study was conducted with one source of RAP: RAP-TH 10 (Trunk Highway at 10 mi location) collected by the Minnesota Department of Transportation during earlier research. This selection was made to avoid the problem of RAP variability, which would arise if RAP were collected from several sources or sites. This material was mixed with Class 5 of base aggregates with 50%, 75%, and 100% of RAP. For sample homogeneity, the maximum particle size was recommended to be less than 10% of the mold size; therefore all material greater than 12.5 mm was replaced by other materials that passed through a 12.5-mm sieve and were retained on Sieve No. 4 (4.75 mm). This adjustment was the only one made for aggregate gradation in this stage of the research (*8*). For this kind of RAP, the OMC was 5.5%, and the MDD was 2,124 kg/m^3. For Class 5, the OMC was 6.4%, and the MDD was 2,223 kg/m^3 (*3*).

The M_R test was conducted immediately after sample compaction. The target sample size was 6 in. in diameter and 12 in. in height. The sample was subjected to 1,000 load cycles for preconditioning followed by 30-load sequences as specified by NCHRP 1-28A protocol, Procedure 1A (*6*). The M_R test was conducted inside a triaxial pressure chamber, which could maintain the required confining pressure. These results of the measured M_R were produced earlier by the North Dakota State University, Fargo, research team in cooperation with the Minnesota Department of Transportation, which supplied the material samples. These results were used in the study reported here to compare the measured and predicted values of M_R for the constitutive models under consideration.

The nine prediction models for M_R (Table 1), which were used previously to predict the M_R for a granular base course layer, were considered in the study reported here. A comparison of the measured and predicted M_R values at various percentages of RAP was taken into consideration for the different factors. These factors were water content that varied from OMC −3% to OMC +2%, dry density of the sample that changed from 100% to 90% of MDD, and the F-T cycle, which had not been studied for RAP behavior. The samples were subjected to two cycles of F-T before they were tested to determine the M_R values. The F-T limits were set by freezing samples at −12°F for 24 h and then by thawing them for 24 h at 75°F (*4*). All of these factors were compared under the effect of different percentages of RAP to the equivalent measured M_R samples under the same conditions.

ANALYSIS OF RESULTS

Six models were rejected after comparisons of the predicted and measured values of M_R at the three percentages of RAP (50%, 75%, and 100%) with the interaction of other factors (e.g., water content, dry density, F-T conditions) (Table 2). Only three of the nine models investigated were considered applicable for RAP behavior. They were the Pezo, MEPDG, and Witczak models. These results were attributed to the relative closeness of the regression lines, obtained from these models, to the equity line (*14*). The implication was that the best prediction of the M_R values might be obtained with these models (Figures 1–3). This finding was confirmed by the results of the calculated R^2, because these three models yielded the highest values for all tested conditions (Tables 3–5).

This research constituted the first stage in the analysis of RAP concept behavior in the base course layer. A second stage was performed to assess the best fit of the three models chosen on RAP behavior and took into consideration all the interactions in the study at the three concentrations of RAP. This second stage was carried out through a comparison of each multiple regression constant K value of each model under the effect of tested conditions at different RAP percentages to understand the possible changes, if any, of each K value.

Witczak Model Parametric Analysis

On the basis of the Witczak model equation, K_{23} was directly related to M_R. As shown in Figure 4, K_{23} increased for 75% and 100% of RAP. It reached its maximum value at OMC and increased enormously when MDD decreased from 100% to 90% for all RAP percentages. However, the K_{23} value differed completely under the effect of F-T, because it decreased in general for all RAP percentages and increased after it exceeded the OMC. In general, K_{23} was at its highest values at 100% RAP under the effect of all tested conditions, which resulted in an increase in M_R.

The same behavior was noticed for K_{24} under the effect of the water content as it reached its maximum value at OMC for all RAP percentages. No general trend was observed for K_{24} under the effect of F-T, and its values were almost the same for all RAP percentages but with different behavior for each percent. The effect of decreases in the MDD was to increase slightly the K_{24} values. This increase continued with increases in the water content. However, the percentage of RAP did not have a remarkable significance on the K_{24} values in general under the effect of all the factors studied. The effect of K_{24} on the M_R differed according to the value under the power, because the M_R might increase or decrease, as shown in the Witczak model equation in Table 1.

The effect of K_{25} on the M_R was directly proportional: the lower the K_{25}, the lower the M_R, as shown in the equation in Table 1. Under the effect of water content, K_{25} reached its minimum value at the OMC, especially in the 75% and 100% RAP cases. No difference in the K_{25} was noticed under the effect of decreases in the MDD. However, it tended to show a rather linear trend with water content variations. The effect of F-T on K_{25} showed that it significantly increased and was almost the same for all RAP percentages without a definite behavior for water content variations. In general, K_{25} affected the M_R negatively, especially under the effect of water content and decreases in the MDD. However, this negative effect was minimized by the effect of F-T.

The study did not consider the effects of the tested factors for parameters K_{26} and K_{27}. After trial-and-error assumptions of different values were made for each parameter at various percentages of RAP, it was found that $K_{26} = -5$ and $K_{27} = 5$ yielded the highest R^2 for the linear comparison between predicted and measured M_R values. Thus it was assumed that $K_{26} = -5$ and $K_{27} = 5$ for all interactions of the tested factors at all percentages of RAP.

TABLE 2 R^2 Parameter for Six Rejected Models

Water Content (%)	Maximum Dry Density (%)	F-T Condition	Confining Pressure Model	Bulk Stress Model	Bulk and Deviator Stress Model	Bulk and Octahedral Shear Stress Model	Average Stress Model	General Stress Model
50% RAP								
OMC–3	100	No	.81	.38	.94	.94	.32	.98
OMC–2	100	No	.84	.55	.72	.72	.01	.86
OMC–1	100	No	.88	.44	.91	.91	.22	.96
OMC	100	No	.94	.53	.87	.87	.02	.96
OMC+1	100	No	.88	.48	.82	.82	.02	.92
OMC+2	100	No	.91	.80	.88	.88	.02	.04
OMC–2	90	No	.85	.37	.88	.88	.17	.95
OMC	90	No	.85	.43	.86	.86	.17	.70
OMC+2	90	No	.82	.46	.81	.81	.05	.90
OMC	100	Yes	.96	.70	.90	.90	.003	.96
OMC+1	100	Yes	.86	.55	.85	.85	.006	.80
OMC+2	100	Yes	.77	.33	.66	.66	.05	.90
75% RAP								
OMC–3	100	No	.96	.66	.97	.97	.15	.98
OMC–2	100	No	.91	.50	.96	.96	.30	.98
OMC–1	100	No	.81	.32	.91	.91	.34	.98
OMC	100	No	.93	.62	.87	.87	0.00	.93
OMC+1	100	No	.93	.81	.88	.88	.01	.96
OMC+2	100	No	.92	.76	.90	.90	.08	.95
OMC	100	Yes	.95	.57	.85	.85	.008	.96
OMC+2	100	Yes	.95	.65	.92	.92	.06	.97
100% RAP								
OMC–3	100	No	.77	.40	.93	.93	.22	0.00
OMC–2	100	No	.82	.40	.97	.97	.31	.81
OMC–1	100	No	.76	.29	.91	.91	.30	.27
OMC	100	No	.86	.40	.86	.86	.04	.37
OMC+1	100	No	.92	.51	.84	.84	.03	.46
OMC+2	100	No	.94	.66	.89	.89	.03	.63
OMC–2	90	No	.74	.29	.88	.88	.33	.93
OMC	90	No	.69	.16	.81	.81	.03	.92
OMC+2	90	No	.65	.24	.71	.71	.21	.91
OMC	100	Yes	.83	.41	.73	.73	.04	.91
OMC+1	100	Yes	.86	.42	.77	.77	.03	.92
OMC+2	100	Yes	.66	.19	.86	.86	.24	.93

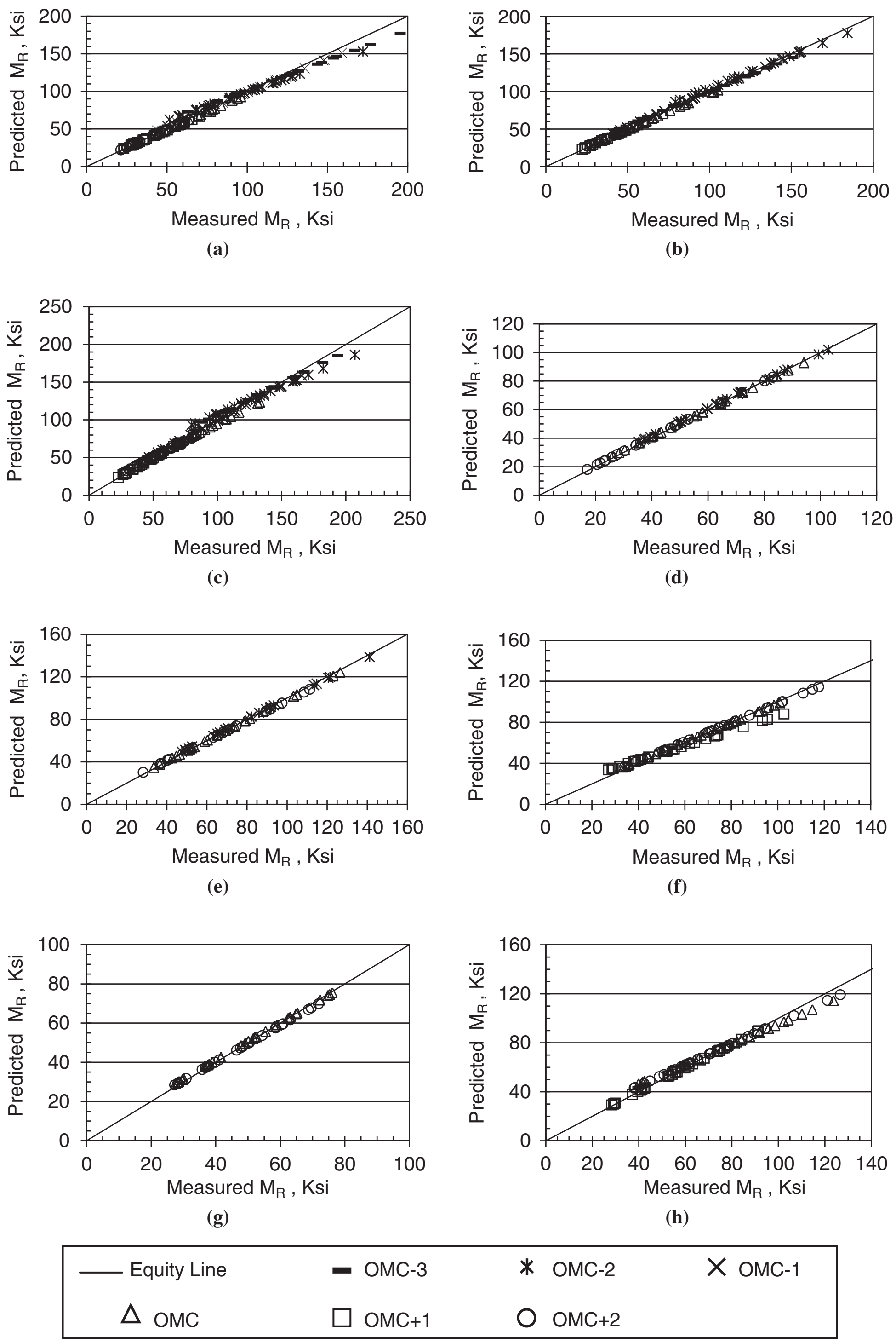

FIGURE 1 Comparison of measured and predicted M_R values of Witczak model: water content effect at (*a*) 50% RAP, (*b*) 75% RAP, and (*c*) 100% RAP; 90% MDD at (*d*) 50% RAP and (*e*) 100% RAP; and F-T condition effect at (*f*) 50% RAP, (*g*) 75% RAP, and (*h*) 100% RAP.

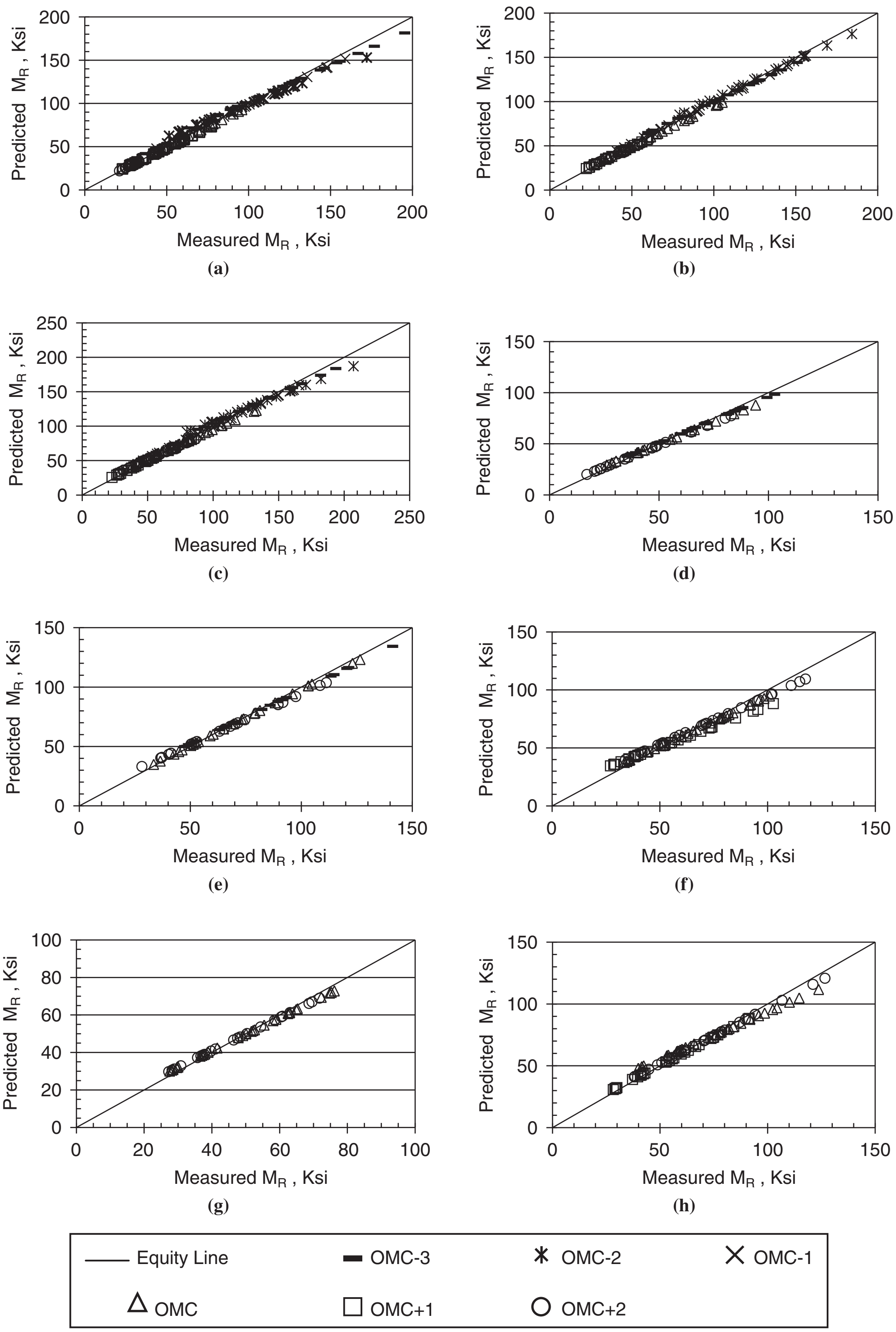

FIGURE 2 Comparison of measured and predicted M_R values of MEPDG model: water content effect at (*a*) 50% RAP, (*b*) 75% RAP, and (*c*) 100% RAP; 90% MDD at (*d*) 50% RAP and (*e*) 100% RAP; and F-T condition at (*f*) 50% RAP, (*g*) 75% RAP, and (*h*) 100% RAP.

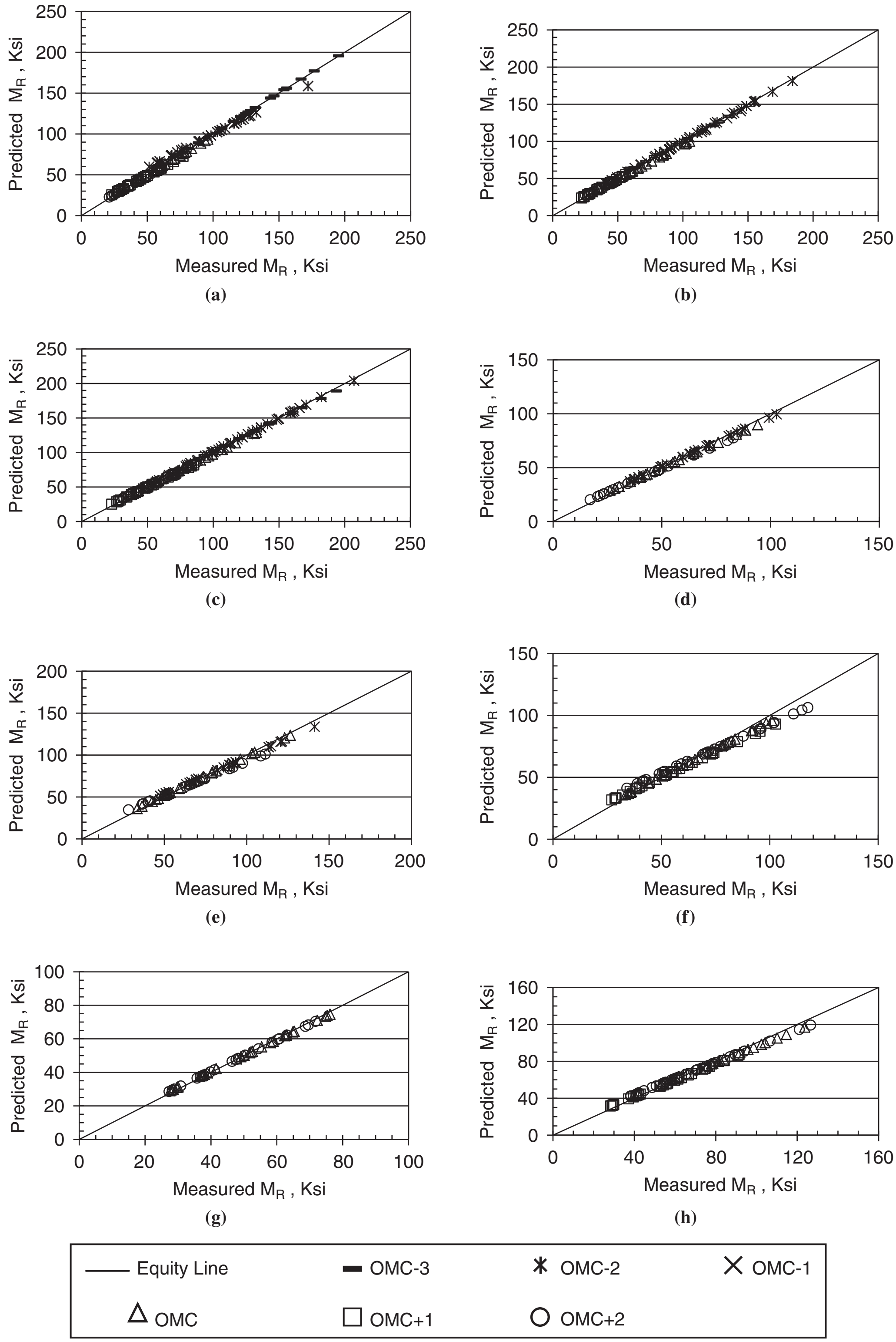

FIGURE 3 Comparison of measured and predicted M_R values of Pezo model: water content effect at (*a*) 50% RAP, (*b*) 75% RAP, and (*c*) 100% RAP; 90% MDD at (*d*) 50% RAP and (*e*) 100% RAP; and F-T condition at (*f*) 50% RAP, (*g*) 75% RAP, and (*h*) 100% RAP.

TABLE 3 R^2 Parameter for Water Content Effect on RAP Approved Models

Water Content (%)	50% RAP Pezo Model (Figure 3*a*)	50% RAP MEPDG Model (Figure 2*a*)	50% RAP Witczak Model (Figure 1*a*)	75% RAP Pezo Model (Figure 3*b*)	75% RAP MEPDG Model (Figure 2*b*)	75% RAP Witczak Model (Figure 1*b*)	100% RAP Pezo Model (Figure 3*c*)	100% RAP MEPDG Model (Figure 2*c*)	100% RAP Witczak Model (Figure 1*c*)
OMC–3	.99	.90	.89	.98	.93	.93	.95	.89	.87
OMC–2	.84	.78	.80	.98	.92	.90	.96	.82	.79
OMC–1	.96	.94	.95	.97	.96	.95	.97	.94	.92
OMC	.96	.95	.97	.93	.96	.98	.96	.91	.91
OMC+1	.91	.86	.91	.94	.94	.97	.93	.95	.98
OMC+2	.91	.92	.96	.92	.89	.93	.94	.89	.90

TABLE 4 R^2 Parameter for 90% MDD Effect on RAP Approved Models

Water Content (%)	50% RAP Pezo Model (Figure 3*d*)	50% RAP MEPDG Model (Figure 2*d*)	50% RAP Witczak Model (Figure 1*d*)	100% RAP Pezo Model (Figure 3*e*)	100% RAP MEPDG Model (Figure 2*e*)	100% RAP Witczak Model (Figure 1*e*)
OMC–2	.95	.94	.96	.93	.94	.96
OMC	.93	.91	.95	.94	.91	.94
OMC+2	.89	.87	.90	.83	.81	.88

TABLE 5 R^2 Parameter for F-T Effect on RAP Approved Models

Water Content (%)	50% RAP Pezo Model (Figure 3*f*)	50% RAP MEPDG Model (Figure 2*f*)	50% RAP Witczak Model (Figure 1*f*)	75% RAP Pezo Model (Figure 3*g*)	75% RAP MEPDG Model (Figure 2*g*)	75% RAP Witczak Model (Figure 1*g*)	100% RAP Pezo Model (Figure 3*h*)	100% RAP MEPDG Model (Figure 2*h*)	100% RAP Witczak Model (Figure 1*h*)
OMC	.96	.93	.96	.96	.94	.97	.87	.80	.82
OMC+1	.88	.82	.80	NA	NA	NA	.90	.95	.98
OMC+2	.83	.85	.91	.96	.93	.87	.93	.93	.87

NOTE: NA = not available.

MEPDG Model Parameter Analysis

From the equation in the MEPDG model, it was clear that K_{20} was directly related to M_R. In general, K_{20} decreased with increases in the water content for all RAP percentages, with slightly higher values at 100% RAP (Figure 5). The effect of decreases in the MDD decreased K_{20} slightly, especially at water contents less than the OMC. K_{20} also had higher values at higher percentages of RAP. F-T cycles affected K_{20} negatively, especially at OMC-1 for all percentages of RAP. In general, K_{20} affected all of the results of the tested conditions negatively, especially when the water content exceeded the OMC. K_{20} had a positive effect when the RAP percentage increased.

For all RAP percentages, K_{21} reached its maximum value when the water content was much closer to the OMC (Figure 5). The percentage of RAP did not have a large effect on K_{21} values. The effects of 90% MDD and F-T cycles on K_{21} values were not significant. There was no general trend for the interaction between these factors and water content. K_{21} was almost the same for all RAP percentages. This parameter apparently was affected only by variations in the water content. The effect of K_{21} on the M_R was not clear, because it depended on the value under the power, as shown in the MEPDG model equation in Table 1.

The K_{22} parameter reached its minimum values when water content approached the OMC for all percentages of RAP regardless of level. The absolute values of K_{22} slightly increased, however, under the effect of decreases in the MDD; the significance of the percentage of RAP increased at higher percentages, especially at lower water contents. The F-T cycles had no significant effect on K_{22} for all RAP percentages. In general, the parameters of this model were affected most by variations in water content, a little by decreases in MDD, and almost not at all by F-T cycles at all percentages of RAP. The parameters were not remarkably affected by increases in the percentage of RAP.

Pezo Model Parameter Analysis

K_{11} was directly proportional to M_R. Figure 6 clearly shows that K_{11} decreased as the water content and the percentage of RAP increased. Both factors (90% MDD and F-T cycles) affected K_{11} negatively with variations in the water content. This effect was especially

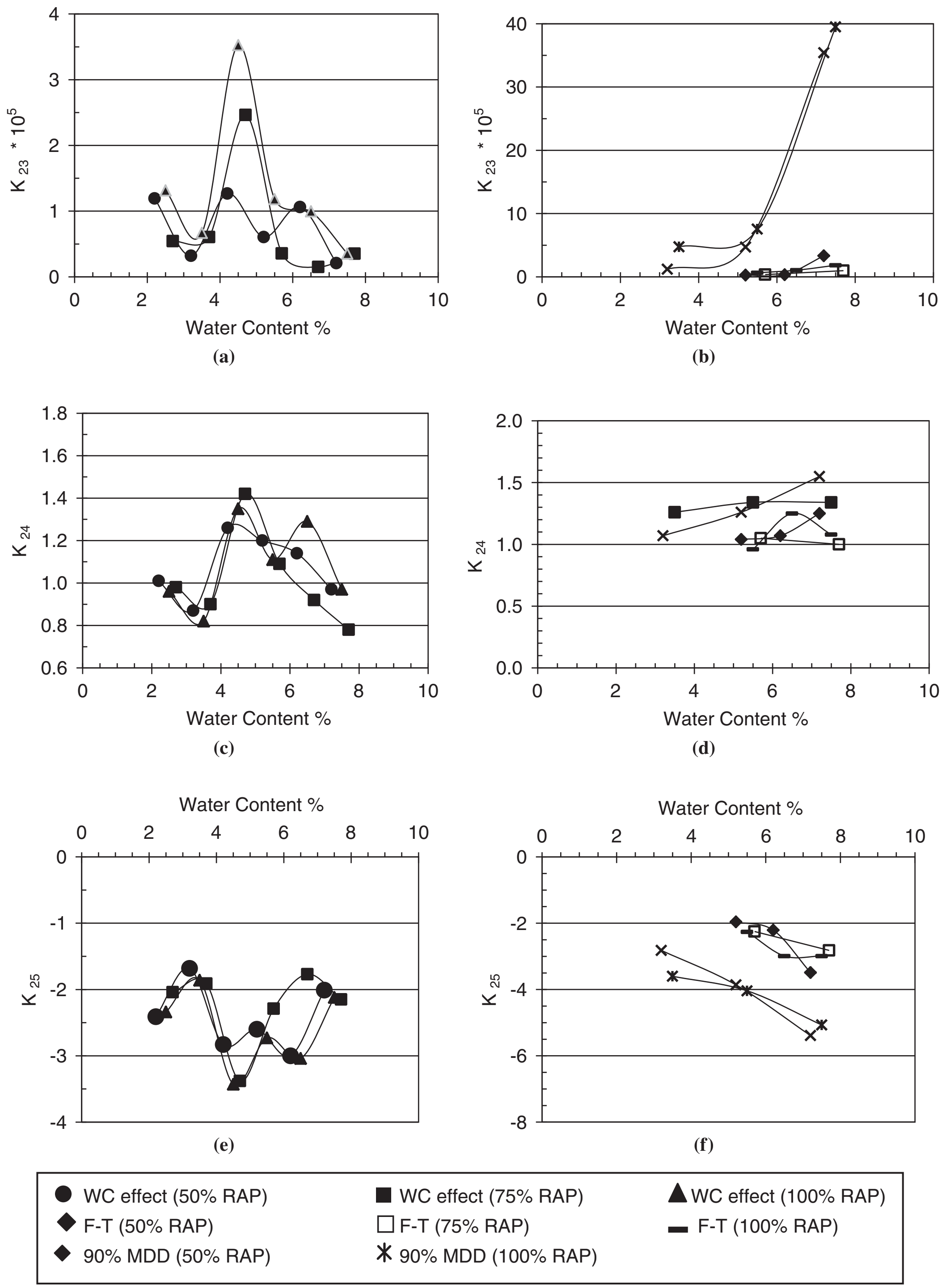

FIGURE 4 Analysis of K parameters for Witczak model parameters under tested factors: (*a*) water content effect on (*a*) K_{23}, (*c*) K_{24}, and (*e*) K_{25}; F-T and 90% MDD effect on (*b*) K_{23}, (*d*) K_{24}, and (*f*) K_{25}.

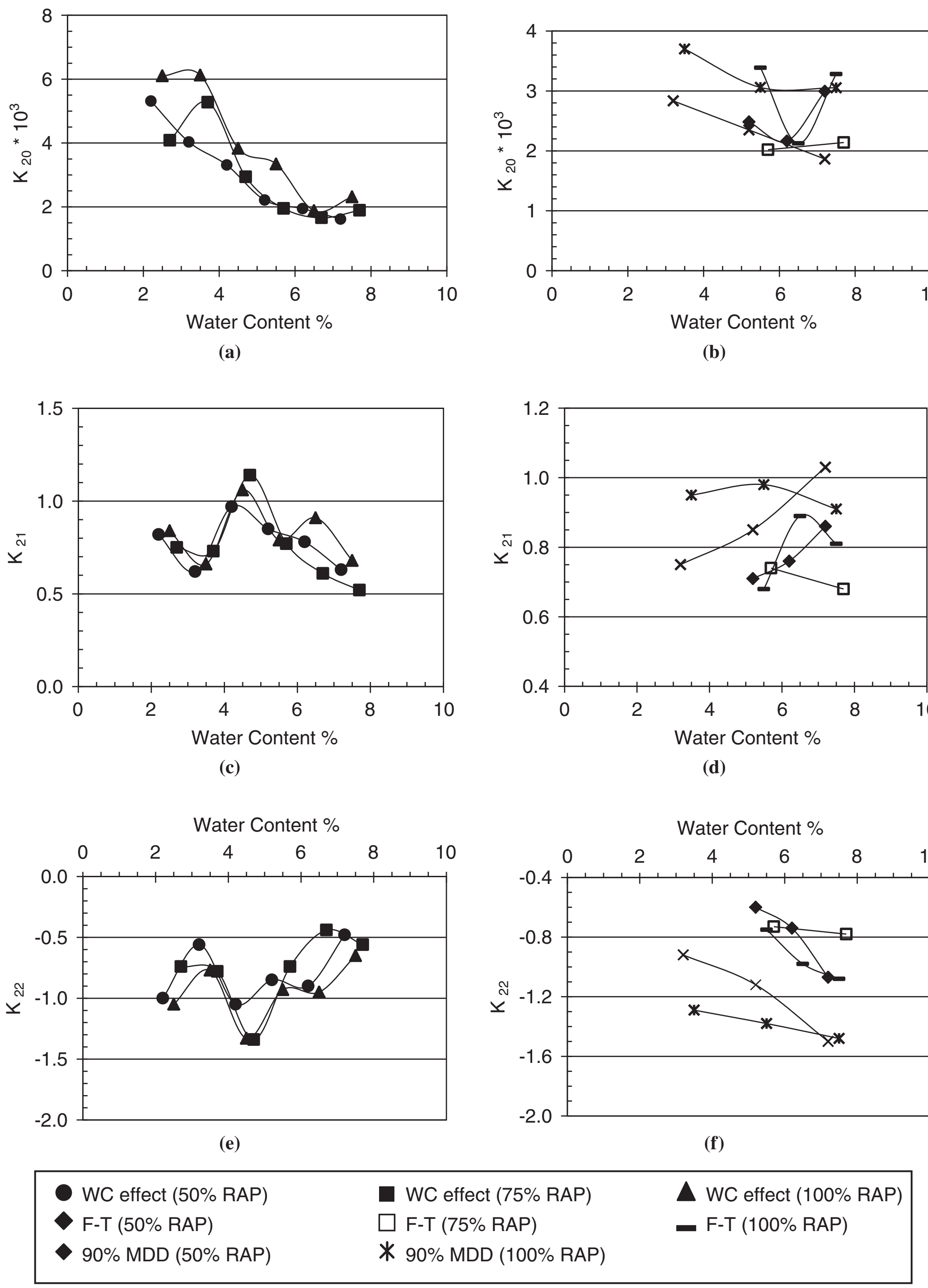

FIGURE 5 Analysis of *K* parameters for MEPDG model parameters under tested factors: (*a*) water content effect on (*a*) K_{20}, (*c*) K_{21}, and (*e*) K_{22}; F-T and 90% MDD effect on (*b*) K_{20}, (*d*) K_{21}, and (*f*) K_{22}.

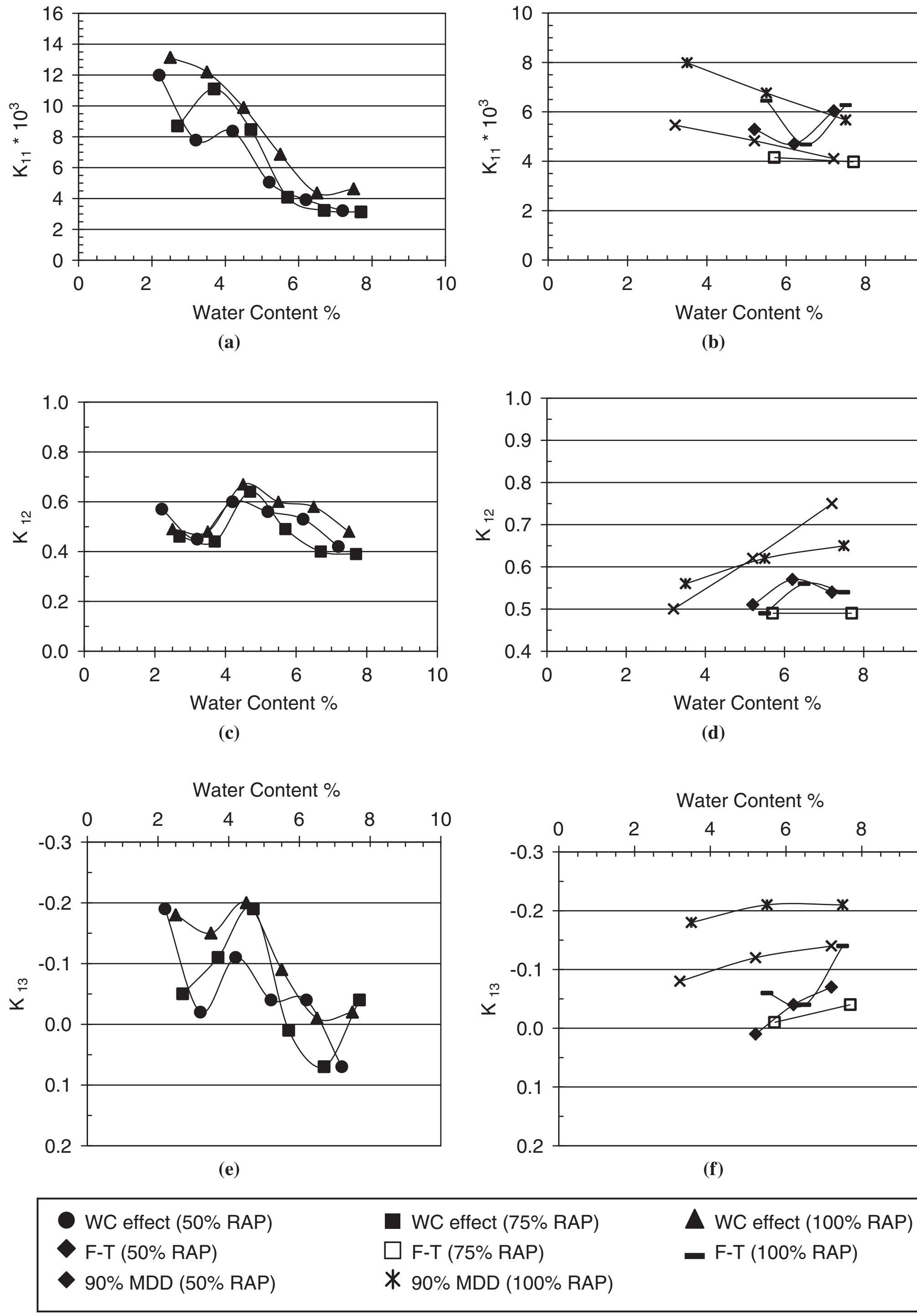

FIGURE 6 Analysis of *K* parameters for Pezo model parameters under tested factors: water content effect on (*a*) K_{11}, (*c*) K_{12}, and (*e*) K_{13}; F-T and 90% MDD effect on (*b*) K_{11}, (*d*) K_{12}, and (*f*) K_{13}.

noticeable for 90% MDD, because the interaction with the water content was more obvious than it was for the F-T cycles. In general, all of the tested factors affected K_{11} values negatively with consequently negative effects on the M_R values as shown in the Pezo model equation in Table 1.

The K_{12} parameter reached its maximum values at the OMC without significance with respect to the percentage of RAP (Figure 6*c*). In its interactions with the other factors, K_{12} increased slightly, especially with 90% MDD and water content (Figure 6*d*). Almost no significant effects were noticed during the application of F-T cycles on the K_{12} parameter alone.

K_{13} reached its minimum value when the water content approached the value of the OMC (Figure 6*e*). The percentage of RAP had little significance. Slight decreases in the MDD decreased K_{13} slightly with the significance of the percentage of RAP. F-T cycles had almost no significant effect on K_{13} at all RAP percentages. In general, the parameters of this model did not exhibit a well-defined behavioral trend under the effect of the tested factors, except that K_{11} was affected negatively by the tested conditions and thus had a negative effect on the M_R values.

CONCLUSIONS

This research study comprised a two-stage analysis. The first stage involved a statistical analysis of the nine M_R prediction models that have been used for granular materials to study the effect of RAP under some field and environmental conditions (e.g., water content, dry density, F-T cycles) and at three percentages of RAP (50%, 75%, and 100%). The analysis in this first stage was achieved through a comparison of the predicted and measured M_R values under the above-mentioned testing conditions. This analysis proceeded through the calculation of the dimensionless multiple regression constant K parameters in each model to determine their value.

Through these comparisons, three models were chosen (Figures 1–3) on the basis of the highest R^2 and the least deviation from the equity line of measured and predicted M_R values. These three models were considered the best fit for RAP behavior under the tested conditions. It was believed, however, that another analysis was needed to confirm these results before a final selection could be made of the best-fit models for RAP behavior. Thus a second stage of analysis was carried out on the three models to compare each K (multiple regression parameter) under the effect of each condition of the tested factors and at all RAP percentages for each model.

As Figures 4–6 show, the MEPDG model gave a better physical description of the results than the other two models. In general, the parameters of the MEPDG model were greatly affected by water content variation, slightly affected when the MDD decreased, and affected almost not at all by F-T cycles at all percentages of RAP. This model's parameters were not greatly affected by increases in the percentage of RAP. The model did, in general, give the best prediction of M_R values at 75% RAP.

ACKNOWLEDGMENTS

The research presented in this paper has its basis, in part, in data collected for a research project supported by the Minnesota Department of Transportation. The authors acknowledge the Minnesota Department of Transportation also for its partial support and provision of material that has its basis in work supported by the National Science Foundation. The original measured data were presented in the PhD dissertation of Mohamed Attia (*4*).

REFERENCES

1. *User Guidelines: Reclaimed Asphalt Pavement, Granular Base.* FHWA, Turner-Fairbank Highway Research Center, McLean, Va. http://www.tfhrc.gov/hnr2U/recycle/waste/rap 134.htm. Accessed July 2008.
2. Huang, Y. *Pavement Analysis and Design.* Prentice Hall, Inc., Englewood Cliffs, N.J., 1993.
3. Attia, M. I. E., and M. Abdelrahman. Effect of State of Stress on the Resilient Modulus of Base Layer Containing Reclaimed Asphalt Pavement. *International Journal of Road Materials and Pavement Design,* Vol. 12, No. 1, 2011, pp. 79–97.
4. Attia, M. I. E. *RAP Structural Behavior as Pavement Base Layer.* PhD dissertation. North Dakota State University, Fargo, 2010.
5. Itani, S. Y. *Behavior of Base Materials Containing Large-Sized Particles.* PhD dissertation. Georgia Institute of Technology, Atlanta, 1990.
6. Witczak, M. W. Harmonized Test Methods for Laboratory Determination of Resilient Modulus for Flexible Pavement Design. NCHRP Project l-28A. Transportation Research Board of the National Academies, Washington, D.C., 2003.
7. Alam, T. B. *Structural Properties of Recycled Asphalt Pavement as a Base Layer.* MS thesis. North Dakota State University, Fargo, 2008.
8. Kim, W., and J. F. Labuz. Resilient Modulus and Strength of Base Course with Recycled Bituminous. Report MN/RC-2007-05. Minnesota Department of Transportation, Saint Paul, 2007.
9. Uzan, J. Characterization of Granular Materials. In *Transportation Research Record 1022,* TRB, National Research Council, Washington, D.C., 1985, pp. 52–59.
10. Witczak, M. W., and J. Uzan. The Universal Airport Pavement Design System. Report I of V: Granular Material Characterization. University of Maryland, College Park, 1988.
11. Pezo, R. F. A General Method of Reporting Resilient Modulus Tests of Soils: A Pavement Engineer's Point of View. Presented at 72nd Annual Meeting of the Transportation Research Board, Washington D.C., 1993.
12. Tam, W. A., and S. F. Brown. Use of the Falling Weight Deflectometer for in Situ Evaluation of Granular Materials in Pavements. *Proc., 14th Australian Road Research Board Conference,* Canberra, Vol. 14, Part 5, 1988, pp. 155–163.
13. Witczak, M. W., D. Andrei, and W. N. Houston. *Guide for Mechanistic–Empirical Design of New and Rehabilitated Pavement Structures.* Appendix DD-l: Resilient Modulus as Function of Soil Moisture Summary of Predictive Models. Final report, NCHRP Project 1-37A. Transportation Research Board of the National Academies, Washington, D.C., 2000.
14. Attia, M. I. E., and M. Abdelrahman. Predicting the Resilient Modulus of Base Layer Containing Reclaimed Asphalt Pavement. Presented at 88th Annual Meeting of the Transportation Research Board, Washington, D.C., 2009.

Any opinions, findings, and conclusions or recommendations expressed in this material are those of the authors and do not necessarily reflect the views of the National Science Foundation.

The Characteristics of Nonasphalt Components of Asphalt Paving Mixtures Committee peer-reviewed this paper.